PERGAMON

Microelectronics Reliability 42 (2002) 597–605

MICROELECTRONICS RELIABILITY

www.elsevier.com/locate/microrel

Defects in silicon oxynitride gate dielectric films

Hei Wong [a,*], V.A. Gritsenko [b]

[a] Department of Electronic Engineering, City University of Hong Kong, City U, 83 Tat Chee Avenue, Kowloon, Hong Kong
[b] Institute of Semiconductor Physics, Novosibirsk 630090, Russia

Received 4 December 2001

Abstract

As the aggressive scaling of the metal-oxide-semiconductor structure continues, new reliability challenges in gate dielectric materials now came across as the gate dielectric thickness will be further down scaled to its technological constraint (< 3 nm). Since the interface thickness and the capture cross-section of dielectric traps are not scalable, the nano device structures and the giga-scale circuit architectures call for a fabrication process with ultra-high uniformity and repeatability for devices. These put strengthen constraints on the trap density and chemical composition fluctuations of the gate dielectric materials. This paper reviews several important issues of the dielectric traps in oxynitride. Particularly, the paramagnetic defects (≡Si$^{\bullet}$, ≡Si—O—O$^{\bullet}$, ≡$Si_2N^{\bullet}$), diamagnetic defects (≡Si—Si≡, =N—H), dicoordinated Si center (=Si:) and neutral defects (≡SiO$^{\bullet}$, ≡SiOH, ≡Si—O—O—Si≡) are discussed in detail based on both the experimental and simulation results.

1. Introduction

As the aggressive scaling of the metal-oxide-semiconductor (MOS) structure goes on, new reliability challenges in gate dielectric materials now came across [1–5] as the gate dielectric thickness will be further down scaled to less than 3 nm in the nanoscale devices. Although preparation of 1.3 nm ultra-thin gate oxide has been attempted recently by a research group of Bell Laboratories [1], reliability study conducted by Degraeve, Kaczer and Groeseneken shows that an oxide films below 2.5 nm are not good enough because the characteristics have wider statistical spreads and depend more stronger on the temperature [2].

The gate dielectric reliability becomes crucial because the interface thickness and the trap capture cross-section are not scalable. In conventional oxide, the interface layer, in the form of suboxide, is about 5 Å thick and most of the oxide traps are found in this transition region. It was found experimentally that the cross-section for the capture of charge carrier (σ) in oxide could be as large as 10^{-14} cm^2. This value corresponds to an effective capture radius of the trap $R = \sqrt{\sigma/\pi}$ of about 5.6 Å. These parameters are the technological limits of the thickness of oxide film. On the other hand, the retention time requirement for memory is generally over 10 years [5]. This requirement calls for a very low leakage tunnel oxide. However in very thin oxide the interface region and the trap capture cross-sections are so large (when compared to the total oxide thickness) that the interface traps can play a dominant role in the tunneling characteristics. Meanwhile, the number of electrons stored in the floating gate will be scaled down to about 3000 in the 1 Gbit generation [5], any non-uniformity in chemical composition and even surface roughness fluctuation will cause significant charge fluctuation.

To meet this challenge, it is proposed that the amorphous gate silicon dioxide should be replaced by amorphous silicon oxynitride (SiO_xN_y) [6–11] or stacked oxide/nitride dielectric [11]. Silicon nitride prepared by chemical vapor deposition (CVD) is not in good device quality because of the inherent stain in the networks of the amorphous structure [12]. The physical configurations of the network atoms are confined by the bending and stretching forces. It was found that these constraint forces are a linear function of the average coordination number of the atoms [12]. For silicon, the average

* Corresponding author. Tel.: +852-2788-7722; fax: +852-2788-7791.
E-mail address: eehwong@mail.cityu.edu.hk (H. Wong).

0026-2714/02/$ - see front matter
PII: S0026-2714(02)00005-7

coordination number is 2.67 and is optimal because bending forces at oxygen atoms are too weak to function as significant constraints. In silicon nitride the corresponding coordination number is 3.43 and the networks are over-constrained. As the silicon atom stretching constraints are stronger than bending constraints, strain energy will be accumulated along the bending constraints in silicon nitride. The average bond angle is distorted and more defects are resulted. The difference in the bending constraints also results in the poor Si/Si_3N_4 interface. Stacked structure is one of the solutions for making use the advantages of oxide and nitride. Oxide-Nitride-Oxide (ONO) structure has been widely used in the DRAM and EEPROM devices. However, the properties are not good enough for active device applications. Oxynitride is a good approach to improve the dielectric properties. It can be used for bridging the oxide and nitride and their interface to silicon substrate. Fig. 1 compares the atomic structures of silicon oxide and silicon oxynitride. Data in Fig. 1 are taken from Ref. [13]. The Si—O bond length was prolonged and the bonding angle of Si—O—Si become larger and more defects are still expected in oxynitride. The non-stoichiometric silicon oxynitride (with excess silicon) may consist of Si—O, Si—N and Si—Si bonds. To the first order approximation, its bandgap are expected to vary linearly between 5 eV (oxide) and 9 eV (nitride). The grade interface is more effective in reducing the direct tunneling and the interface defect density. These principles can be used to improve the dielectric properties of oxynitride films. Unfortunately, the properties of oxynitride obtained to-date are far below our expectation because of technological problems. The amount of dielectric defects in oxynitride by ammonia (NH_3) nitridation would be very large because of the hydrogen incorporation [6–10]. Although nitrous oxide (N_2O) nitridation seems to have the advantage of low hydrogen content, the amount of nitrogen incorporation, in the range of 2–4 at.%, is still not large enough to improve the hardness for hot carrier irradiation [14]. In addition, this process further suffers from many difficulties. The uniformity and reproducibility between wafers and batches are very poor. Moreover, thermodynamically, nitridation of oxide is much difficult than silicon oxidation even at high temperature. The worst of it is that the defect density is not minimized. Instead, the defect origins are almost three fold: the oxide and nitride defects and their new variants can be found in the oxynitride. The paper reviews several important issues of the dielectric traps in oxynitride. Particularly, the paramagnetic defects (≡Si•, ≡Si—O—O•, $\equiv Si_2N^{\bullet}$), diamagnetic defects (≡Si—Si≡, =N—H), dicoordinated Si center (=Si:) and neutral defects (≡SiO•, =Si:, ≡SiOH, ≡Si—O—O—Si≡) are discussed in detail based on both the experimental and simulation results. A new oxynitride preparation method with low hydrogen content and high nitrogen content is proposed.

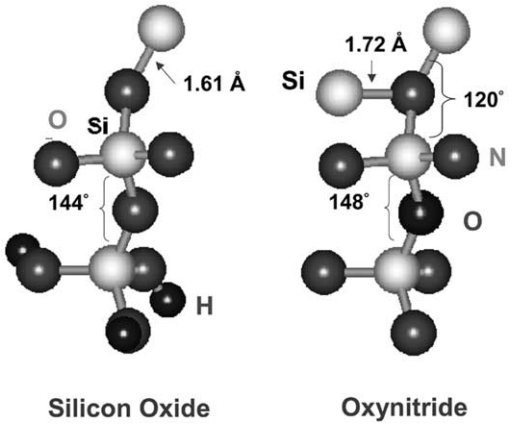

Fig. 1. Atomic structure of silicon oxide and silicon oxynitride.

2. Trap classifications

The electronic quality of a gate dielectric film is governed by the neutral and charged electronic defects. These defects could be physical in several forms of non-bridging or dangling silicon and oxygen bonds. Interstitial or bonded impurities can also serves as the electronic trap centers. From physical point of view, the dangling bonds and the impurities modify the local potentials around these sites. As a result, the bound state solutions to the Schrödinger equation for electron and hole in these sites may be significant. The conduction-band electron and valence-band hole in the dielectric film can then be trapped or captured into these bound states. The known electronic defects in silicon oxide, nitride, and oxynitride can be further classified into the following six groups according to their electronic properties:

(a) Paramagnetic defects such as ≡Si•, ≡Si—O—O•, $\equiv Si_2N^{\bullet}$;
(b) Diamagnetic defects such as ≡Si—Si≡, =N—H, dicoordinated Si center =Si:;
(c) Neutral defects such as ≡SiO•, =Si:, ≡SiOH, ≡Si—O—O—Si≡;
(d) Charged defects such as $\equiv Si^{\bullet}\ {}^{+}Si\equiv$ (*E*'center in SiO_2), $\equiv Si_2N$: (electron captured by $\equiv Si_2N^{\bullet}$ defect in oxynitride);
(e) Intrinsic defects such as ≡Si•, =N—N=, ≡Si—O—O—Si≡, =Si: and
(f) Extrinsic defects such as ≡SiH, $\equiv Si_2NH$, ≡SiOH.

Here the symbols —, = and ≡ in this work represent one single bond, two single bonds and three single bonds, respectively and • denotes one unpaired electron.

3. Trap properties and formation mechanisms

The energy levels of some of the above traps from experiments are listed in Table 1. To have better understanding of these traps, the electronic properties are simulated with MINDO/3. Cluster approximation to study the electronic structure of several different clusters in silicon oxynitride was used. Atomic relaxation in different charge states of defect was considered in the simulation. To simulate the effect of chemical composition on the capturing properties of the $\equiv Si_2N^\bullet$ defect in silicon oxynitride, clusters with different numbers of oxygen and nitrogen atoms, i.e. $^\bullet NSi_2(N_6)SiH_{12}$, $^\bullet NSi_2(N_4O_2)SiH_{10}$ and $^\bullet NSi_2(O_6)H_6$, in the second coordination sphere were considered. For simulation of the Si_3N_4 bulk electronic structure we used the $Si_{20}N_{28}H_{36}$ cluster. The atomic structures of these clusters are shown in Fig. 2 and the simulation results for these traps are illustrated in Fig. 3 [9].

3.1. Paramagnetic defects: $\equiv SiO^\bullet$, $\equiv Si_2N^\bullet$

In silicon oxide, it is well known that oxygen atom with unpaired electron $\equiv SiO^\bullet$ or R-center or non-bridging oxygen hole center (NBOHC) is the well known defect [15]. Electron spin resonance (ESR) and photoluminescence (PL) studies show that this center has energy of 1.9 eV and full width at half maximum (FWHM) of 0.2 eV in oxide. The 1.9 eV PL peak may also due to $\equiv Si_2N^\bullet$ defects in nitride and oxynitride (see Fig. 4). This defect was identified by ESR measurement in Si_3N_4 and SiO_xN_y by Warren et al. [16] and Chaiyasena et al. [17], respectively. This kind of defects becomes more complicated in oxynitride. The silicon atoms in these defects can be randomly coordinated by different number of oxygen and nitrogen atoms, i.e. $O_{3-\beta}N_\beta SiO^\bullet$ or $O_{3-\beta}N_\beta SiN^\bullet$ where $\beta = 0, 1, 2, 3$. As a result, a slight different peak energy from the conventional R-center.

As shown in Fig. 4, the intensity of R-center in oxynitride becomes higher as the oxygen concentration increases because of the high density of $\equiv SiO^\bullet$ defect in high oxygen concentration samples. On the other hand, increase in nitrogen concentration gives rise to the increase of the FWHM and a shift of the peak to lower energy. Depending on the amount of $\equiv SiO^\bullet$ and $\equiv Si_2N^\bullet$ defects, the peak position may vary. A low-energy shift can be observed in high nitrogen concentration in sample because of the increase of $\equiv Si_2N^\bullet$ defects.

Table 1
Catholuminescence and photoluminescence features of the major defects in oxynitride film

Luminescence method	Energy (eV)	Origins
CL	1.9	$O_{3-\beta}N_\beta SiO^\bullet$
CL	2.7	O_2Si:,N_2Si: or NOSi:
CL	3.1–3.6	$N_3Si{-}SiN_3$
CL	4.4–4.7	$\equiv Si{-}S\equiv$, $N_3Si{-}SiN_3$
CL	5.4–5.7	$\equiv SiOO^\bullet$
PL	2.4–3	$\equiv Si{-}Si\equiv$ (electron)
PL	4.4	$=Si$:
PL	5.7–6.3	$\equiv Si{-}Si\equiv$ (hole)

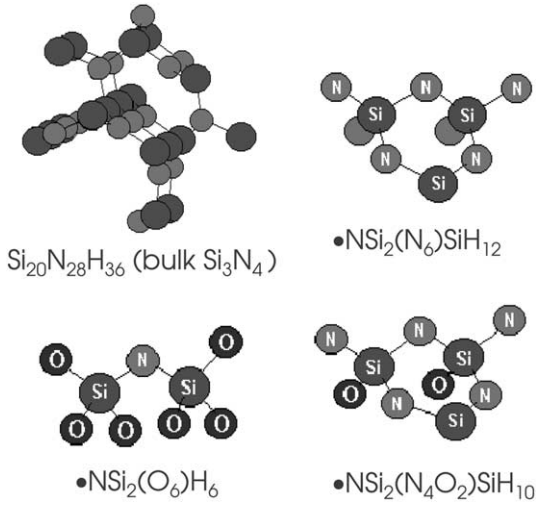

Fig. 2. Clusters used in simulating the defect capturing properties of (a) $Si_{20}N_{28}H_{36}$, (b) $NSi_2(N_6)SiH_{12}$, (c) $^\bullet NSi_2(N_4O_2)$-SiH_{10} and (d) $^\bullet NSi_2(O_6)H_6$.

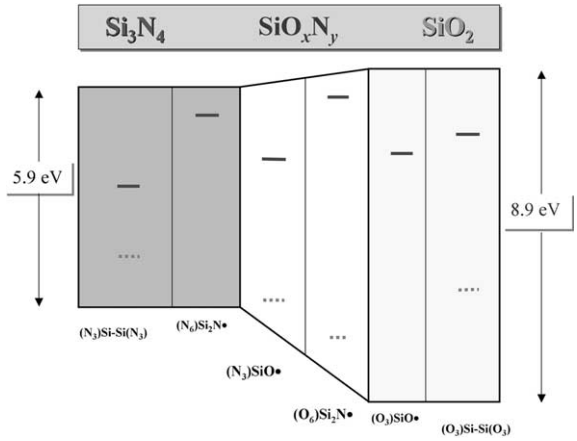

Fig. 3. Calculated energy diagram for the major defects in oxynitride. Similar defects in oxide and nitride are also shown for comparison.

The creation of $\equiv Si_2N^\bullet$ defect in oxynitride could be resulted from the breaking of the $Si_2N{-}H$ or $N{-}N$ bond according to the following reactions

$$\equiv Si_2NH \rightarrow \equiv Si_2N^\bullet + H \quad (1)$$

$$\equiv Si_2N{-}NSi_2\equiv \rightarrow \equiv Si_2N^\bullet + {}^\bullet NSi_2\equiv \quad (2)$$

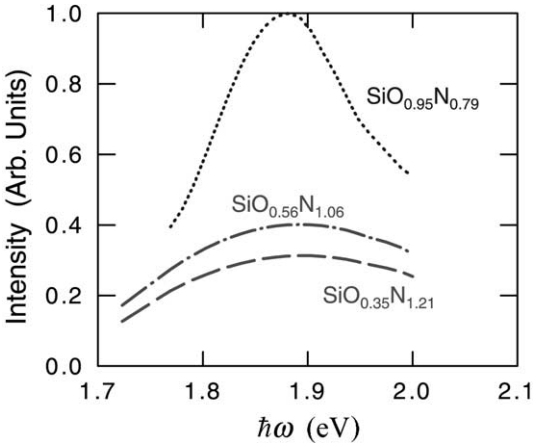

Fig. 4. Cathodoluminescence spectra of SiO_xN_y films with different composition in the visible and near ultraviolet range.

This kind of defect can be removed by re-oxidation, i.e.

$$\equiv Si_2N^{\bullet} + O \rightarrow \equiv Si{-}O{-}Si\equiv + N \quad (3)$$

The oxygen replacement occurs without other atom re-arrangement as the nitrogen atom and the nitrogen defect have the same coordination number.

Fig. 3 shows the calculated energy diagram for $\equiv Si_2N^{\bullet}$ and $\equiv SiO^{\bullet}$ defects in oxynitride. Similar defects in oxide and nitride are also shown for comparison. The obtained values of the energy gain for the capture of electron from the bottom of the conduction band (E_c) is about 1.0 eV. That is the thermal delocalization electron trap energy is about 1.0 eV. However, the capture of hole from the top of the valence band (E_v) is energetically unfavorable. In addition, simulation results also show that the electron trap energy is weakly depends on the cluster chemical composition. The energy gain results indicated that the $\equiv Si_2N^{\bullet}$ defect in silicon nitride and oxynitride with high concentration of nitrogen cannot capture a hole but an electron. Our results also agree with Powell and Robertson [18] that the negatively charged nitrogen defect $\equiv Si_2N:$ can be a hole trap. We also rule out the possibility that the neutral $\equiv Si_2N^{\bullet}$ defect may also act as a hole trap in Si_3N_4 which was proposed by Kirk [19]. Simulation of the neutral $\equiv Si_2N^{\bullet}$ defect shows that unpaired electron is localized for all considered clusters in the N $2p_{\pi}$ nitrogen non-bonding orbital which is oriented normally to the Si_2N plane. The captured electron is localized in the N $2p_{\pi}$ non-bonding orbital of the $\equiv Si_2N^{\bullet}$ defect (see Fig. 5).

This result agrees with the previous theoretical simulation of this defect in silicon nitride [20,21]. As obtained in Ref. [16] for the $\equiv Si_2N^{\bullet}$ defect in Si_3N_4, the wavefunction of the unpaired electron consists from 90% of p-type and 10% of s-type atomic functions.

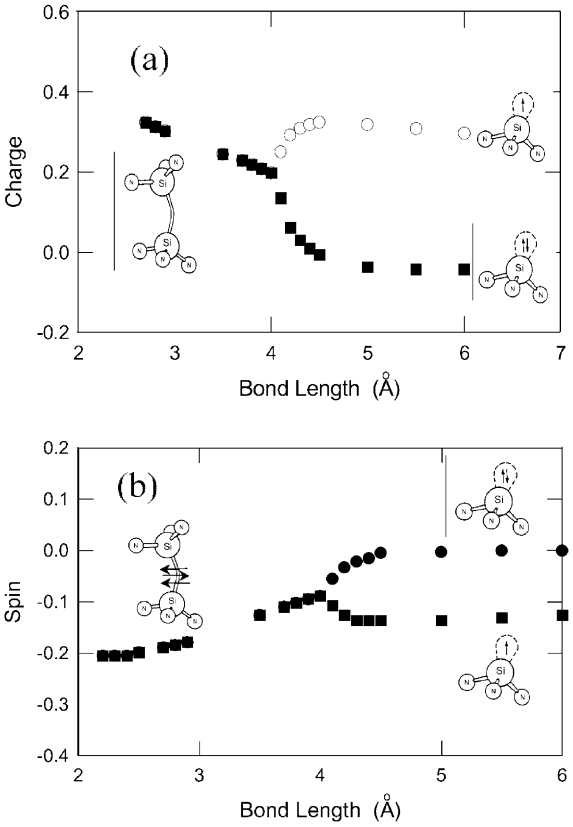

Fig. 5. Model of three-fold coordinated nitrogen atom as an electron trap in silicon nitride and oxynitride (a) capture of electron and (b) capture of hole.

Similar result was also obtained from the analysis of ESR signal hyperfine splitting in oxynitride [20]. On the other hand, simulation results also suggest that the electron localization by the $\equiv Si_2N^{\bullet}$ defect will result in spin dissipation. This effect was experimentally observed earlier [20]. Electron localization results in the transfer of paramagnetic defect $\equiv Si_2N^{\bullet}$ to diamagnetic defect $\equiv Si_2N:$. The corresponding model is picturized in Fig. 5.

The precursor of $\equiv SiO^{\bullet}$ defect can be the peroxyl linkage ($\equiv Si{-}O{-}O{-}Si\equiv$) in silicon oxide. The silicon to silicon distance with a peroxyl contented network could be as large as 3.47 Å which is significantly larger than that value of silicon oxide and oxynitride, thus this linkage could be readily broken according to the following reaction:

$$\equiv Si{-}O{-}O{-}Si\equiv \rightarrow 2\equiv Si{-}O^{\bullet} \quad (4)$$

The peroxy radical may be generated during oxidation or thermal annealing

$$\equiv Si^{\bullet}(E'\text{center}) + O_2 \rightarrow \equiv Si{-}O{-}O^{\bullet} \quad (5)$$

$$\equiv Si{-}O^{\bullet} + O \rightarrow \equiv Si{-}O{-}O^{\bullet} \quad (6)$$

The experimental observed optical absorption at 5.3 ± 0.2 eV [22] is attributed to the peroxyl radical $=SiOO^{\bullet}$ oxide. In oxynitride the intensity of this peak increases with the oxygen concentration.

3.2. Paramagnetic defects $\equiv Si^{\bullet}$

It is well known that the P_b center ($\equiv Si^{\bullet}$) is the major source of surface states at the Si/SiO_2 interface [23–25]. A P_b center is a threefold-coordinated silicon atom with an unpaired electron and is an electron and hole amphoteric surface centers at the Si/SiO_2 interface. With thermal nitridation, the density of the P_b center was reduced from 2×10^{12} cm^{-2} to a value below 10^{11} cm^{-2} [26]. This is a good interface property for MOS devices application.

According to the Mott rule, the interface state creations being suppressed during the SiO_2 nitridation can be explained by the reaction of nitrogen atoms with the Si—Si bonds in SiO_2 and P_b centers on the silicon surface according to the following reaction:

$$\equiv Si{-}Si\equiv + N + {}^{\bullet}Si\equiv \rightarrow \equiv Si_3N \tag{7}$$

With this reaction, the nitrogen atom incorporation during the nitridation accompanies the removal of Si—Si bonds and the silicon dangling bonds ($\equiv Si^{\bullet}$). The resulting species are chemically and electrically stable.

3.3. Diamagnetic defect $\equiv Si{-}Si\equiv$

The creation of Si—Si bonds in the oxynitride can be understood on the atomic scale by Mott rule which can be used to describe the short-range order in silicon oxide, silicon nitride, and silicon oxynitride. Mott rule is

$$C_N = 8 - n \tag{8}$$

where C_N is the coordination number and n is the number of electrons taking part in the chemical bond. The number of valence electrons for Si, O and N are 4, 6 and 5, respectively. According to (8) silicon, oxygen and nitrogen atoms in silicon, silicon dioxide and silicon nitride have 4, 2 and 3 neighbor atoms, respectively. It was obtained quantitatively that the short-range order of silicon oxynitride of different composition can also be described by Mott rule. Since an N atom in Si_3N_4 is coordinated by three Si atoms, and an O atom in SiO_2 is coordinated by two Si atoms, substitution of N by O accompanies the creation of a silicon dangling bond or E′ center $\equiv Si^{\bullet}$, i.e.

$$2 \equiv Si_3N + 2O \rightarrow 2 \equiv Si^{\bullet} + 2 \equiv Si_2O \tag{9}$$

Two such silicon atoms with unpaired electrons results in a creation of Si—Si bond, namely,

$$\equiv Si^{\bullet} + {}^{\bullet}Si\equiv \rightarrow \equiv Si{-}Si\equiv \tag{10}$$

More generally, the reaction describing nitride oxidation can be written as

$$2NSi_3 + O_2 \rightarrow Si{-}Si + 2OSi_2 + N_2 \tag{11}$$

Reaction (11) describes the silicon nitride oxidation in terms of chemical bonds in atomic scale. Silicon–silicon bond ($\equiv Si{-}Si\equiv$) has six external bonds. The six bonds can be connected by O, N and Si with different combination; namely the $\equiv Si{-}Si\equiv$ bond in the samples could be $Si_\nu N_\alpha O_\beta Si{-}SiO_\gamma N_\omega Si_\delta$, where ν, α, β,γ,ω,$\delta = 0$, 1, 2, 3, $\nu + \alpha + \beta = 3$ and $\gamma + \omega + \delta = 3$.

Numerical simulation of the electronic structure of the Si—Si bonds has been made by the semiempirical quantum-chemical method (MINDO/3) where atomic relaxation is also considered [26]. Fig. 6 represents the charge and spins distribution between two silicon atoms of Si—Si bonds in Si_3N_4 with captured electron at Si—Si distance more than 4 Å, asymmetric relaxation of atoms, similar to E′ center in SiO_2, is observed. The simulation shows that Si—Si bonds in nitride, similar to those in oxide film, can capture both holes and electrons. The energy level of the bonding orbit for Si—Si bond is close to the top energy of the valence band (−2.0 eV) and the antibonding orbital level locates near the bottom of the conduction band (−6.5 eV) [22].

This trap give rise to the peak with energy at 3.16, 3.4–3.6 and 4.4–4.7 eV were observed in nitride films in catholuminescence (CL) study [22,27]. Fig. 7 shows the CL results of various oxynitride films. The high-energy peak 4.4 eV, may be due to the $O_3Si{-}SiO_3$ defect (oxygen vacancy). Since the energy difference between σ-bonding and σ^*-antibonding states of Si—Si bond in nitride is 4.6 eV [22], it give rise to 4.7 eV CL peak as a singlet–singlet transition in $N_3Si{-}SiN_3$ bond.

3.4. Dicoordinated Si center ($=Si{:}$)

In silicon oxide, a blue catholuminescence at 2.7 and 4.4 eV PL emission were found and this center was

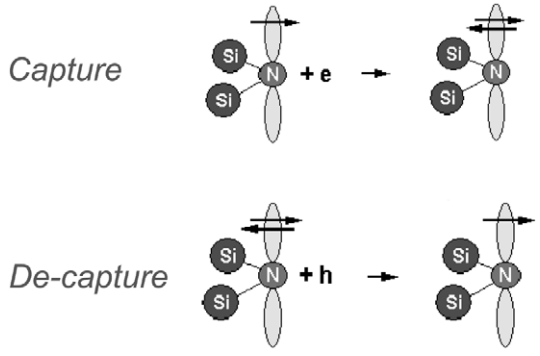

Fig. 6. Charge and spin distributions of silicon atoms for Si—Si bond in Si_3N_4 as a function Si—Si distance.

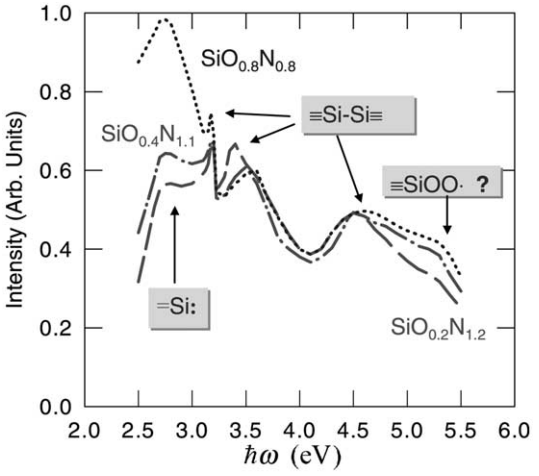

Fig. 7. Cathodoluminescence spectra of various SiO_xN_y films in the visible and near infrared range.

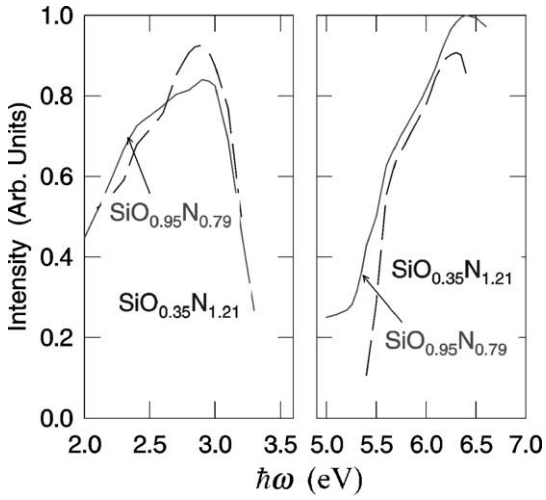

Fig. 8. Photoluminescence spectra of various a-SiO_xN_y films in the visible and ultraviolet range: (a) luminescence with excitation energy of 5.9 eV; (b) the excitation spectra of PL band with energy 2.7 eV.

attributed to the triplet–singlet transitions in two-fold coordinated silicon atom with two unpaired electrons (=Si:) [15]. Numerical simulation of =Si: defect was also performed with the 17-atom $Si_3O_8H_6$ cluster. Results show that the electron capture in =Si: defect is energetically unfavorable. The energy gain for hole capture in this center is −3.2 eV. The hole capture can take place via the reaction given in Fig. 5; i.e., the hole capture in =Si: will result in the creation of paramagnetic two-fold coordinated silicon atom with an unpaired electron. The dicoordinated Si centre should be responsible to the positive charge accumulation in MOS devices during ionizing irradiation. This blue CL peak is also found in oxynitride (see Fig. 8). However, the atomic configuration of this center may be different. In addition to that coordinated by two oxygen atoms (O_2Si:), the dicoordinated Si center in oxynitride can be coordinated by two N atoms (N_2Si:) or and by one Si and one O atom (NOSi:) and small shifts of the PL and CL peaks were found.

3.5. Hydrogen related defects: ≡SiH, ≡Si_2NH and ≡SiOH

Hydrogen is the main chemical impurity in oxide because of residual moisture during oxidation. For oxynitride prepared by ammonia nitridation or by LPCVD or PECVD methods, addition of hydrogen from the gas sources will be incorporated [10,28].

Hydrogen can exist in several forms in the dielectric film. It may be in the molecular form, H—H or in the hydroxyl form, silanol groups (—OH) which are often tied to those preexisting defects as discussed previously, e.g. ≡SiH, ≡SiOH, ≡Si_2NH, ≡Si_2NOH, ≡Si(OH)H, =Si(H)H. These hydrogen bonds are not electronically active as their potential perturbations are too low to have a bound solution for a conduction band electron or valence band hole from the Schrödinger equation. In fact, hydrogen was used to passivate the Si and O dangling bonds in oxide in 1970s. However, the hydrogen bond energy is quite weak, 3.1 eV for Si—H and 4.43 eV for O—H in diatomic molecule. They could be even weaker due to the tight binding of adjacent atoms or over-coordinated network. These bonds can be easily broken under hot electron irradiation or high electric field stressing [29,30] and cause reliability degradation for long-term operation of the devices. In addition, the atomic hydrogen can easily move in the oxide network by defect conversions which do not involve significant network rearrangement. According to Hori et al. [14], the electron injection-induced flatband shift (ΔV_{FB}) of NH_3 nitrided oxide can be approximated by:

$$\Delta V_{FB} = K[H] \tag{12}$$

where K is a constant of about 9.3×10^{-22} V cm^3 and $[H]$ is the hydrogen concentration in the oxynitride. Thus the dielectric trap generation is directly proportional hydrogen concentration and it suggests that the hydrogen atoms in nitrided oxide are appeared in the tied-forms (to the pre-existing defects) as mentioned above.

It was found that ammonia nitridation could induce a lot of N—H bonds and OH bonds and many fixed oxide charges to the oxynitride or nitrided oxide [10]. Although the alternative N_2O nitridation has minimized the hydrogen incorporation, this process still suffers from many difficulties. The uniformity and reproducibility between wafers and batches are very poor. In

addition, thermodynamically, nitridation of oxide is much difficult than silicon oxidation even at high temperature. The nitrogen incorporation is limited to 3 at.% [14]. The nitrogen content is too low to increase the dielectric constant and to improve the dielectric reliability [26,31]. We have also studied the physical structure of N_2O-nitrided oxides [32]. X-ray photoelectron spectroscopy (XPS) measurement indicates that the total nitrogen surface concentration of the prepared "oxynitride" is about $(3 \pm 1) \times 10^{14}$ cm^{-2}. This amount is close to the surface density of a half monolayer of solid and is close to the value of other reports [33–35]. By 200 eV Ar beam sputtering, it was found that the nitrogen distribution is very close (about 5–8 Å) to the Si/dielectric interface. This observation agrees with data obtained by other studies [34,36]. Fig. 9 shows the Si 2p spectra of N_2O oxynitride with thickness of 24 and 16 Å. Si 2p spectra for Si_3N_4 LPCVD bulk oxynitride ($SiO_{0.82}N_{0.90}$) and thermal SiO_2 are also depicted in the figure for comparison. It is noted that the Si 2p XPS spectra of N_2O oxynitride are similar to that of thermal oxide. The Si 2p lines of these samples have the same chemical shift and width. In addition, the O 1s line of N_2O oxynitride is also similar to the thermal oxide ones. The chemical shifts of O 1s and N 1s in various bulk oxynitride ranging from SiO_2 to Si_3N_4 were studied [22]. Compared to these results, it is found that the N_2O oxynitride used in this investigation is in fact a silicon oxide film. The N—O bond, proposed in other experiments [37,38], was not observed in our recently experiment [32].

Hydrogen and nitrogen can be released from the nitride by vacuum annealing. This result could be due to the following reaction

$$2Si_2NH \rightarrow \equiv Si{-}Si \equiv + N_2 + H_2 \quad (13)$$

According to (13), hydrogen will release from silicon nitride due to the broken of NH bonds. This process will accompany with the creation of Si—Si bond. The Si—Si bond creation during the annealing of nitride has been confirmed with the shift of the fundamental absorption to lower energy side. Thus instead of using N_2O, alternative method with proper annealing, for reducing the hydrogen content in oxynitride is possible.

4. An alternative method for oxynitride fabrication

The present oxynitride preparation methods have either drawback of high hydrogen content or low nitrogen content. To overcome these drawbacks, we propose a new method. By re-oxidizing the Si-rich nitride layer, secondary ion mass spectroscopy (SIMS) study reveals that the hydrogen content of nitride film and its interface can be reduced by more than 40%.

Fig. 10 displays the hydrogen profiles of various multi-layer dielectrics. Samples with oxide/oxynitride/oxide structure were fabricated on n-type silicon with <100> orientation and the resistivity is about 4–10 Ω cm. A thin thermal oxide of about 100 Å was first grown with dry oxidation at 850 °C, and then a thin (~130 Å) silicon nitride or silicon-rich nitride layer was deposited on the thermal oxide using low-pressure chemical vapor

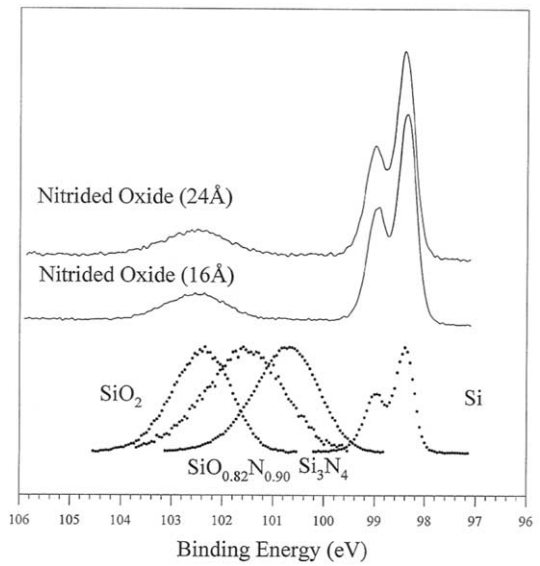

Fig. 9. XPS of Si 2p core level in N_2O-grown oxide, Si_3N_4, LPCVD bulk oxynitride ($SiO_{0.82}N_{0.90}$) and thermal oxide.

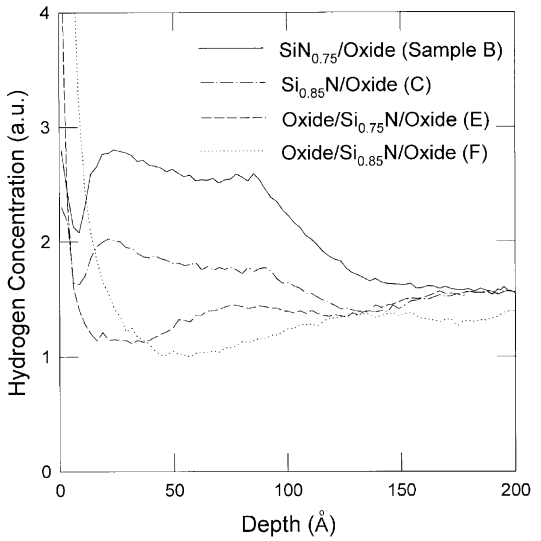

Fig. 10. Hydrogen concentration of samples prepared by oxidation of LPCVD nitride films with different silicon concentrations.

Table 2
Process parameters and thin film properties

Sample	A	B	C	D	E(ONO)	F(ONO)	G(ONO)
Bottom oxide	100	100	100	100	100	100	100
CVD nitride	–	129	128	128	127	124	124
Si/N ratio	–	0.75	0.85	0.90	0.75	0.85	0.90
Top oxide	–	–	–	–	40	40	40

deposition (LPCVD). The chemical sources used for the LPCVD are $SiCl_4$ and NH_3. Details of the process parameters for different samples are listed in Table 2 and other characteristics of the samples can be found in Ref. [39]. The samples were than re-oxidized at 1000 °C for 35 min. It is found that a large number of hydrogen impurities are introduced by the LPCVD process. The hydrogen concentration is the highest near the surface and decrease gradually and then it increases slightly at the interface. Stoichiometric silicon nitride (sample B) has the highest hydrogen content. Silicon rich samples have lower amount of hydrogen. For Si-rich samples with reoxidation (sample F), the hydrogen content decreases by more than 40% and there is no noticeable hydrogen peak can be found at the interface.

In Si-rich samples, the excess silicon atoms should exist in the form of ≡Si-H which can be broken under hot electron or high field stressing and become an electron trap [28,29]. With re-oxidation, oxynitride is formed and the hydrogen concentration can be removed significantly. Si-rich SiO_xN_y consists of Si—O, Si—N and Si—Si bonds and the chemical reactions for the oxidation of silicon-rich nitride could be very complicated. However, the key reactions should involve the following process:

$$2 \equiv Si{-}H + O_2 \rightarrow \equiv Si{-}O{-}Si\equiv + H_2 \quad (14)$$

$$2 \equiv Si_2NH + 2 \equiv SiH + O_2 \rightarrow 2 \equiv Si_3N + H_2O \quad (15)$$

$$2 \equiv SiNH_2 + \equiv Si{-}H + O_2 \rightarrow \equiv SiOH + \equiv Si_2NH + H_2O \quad (16)$$

$$\equiv SiOH + \equiv SiH \rightarrow \equiv Si{-}Si\equiv + H_2O \quad (17)$$

Reactions (14)–(17) describe, on the atomic scale, the possible reactions take place during the silicon nitride oxidation in terms of chemical bonds rearrangement. These reactions involve in the elimination of hydrogen-containing species and results in the removal of potential trap centers.

As mentioned earlier, due to its preparation technique and the large coordination number, the quality of LPCVD silicon nitride is poor and even the worst interface to oxide and silicon and hardly make it to be used in the active device structure. By introducing excess silicon and with re-oxidation, a very good oxynitride can be achieved. The merits of post-CVD oxidation are in threefold. Firstly, it rehears the structural defects in the CVD nitride; secondly, it grades the oxide/CVD nitride interface by making the oxygen and nitrogen profiles more smoother and releases the interface stress and the tunneling current can also be reduced; thirdly, it remove the hydrogen atoms which will be trap centers for dielectric film under hot-carrier irradiation. Note that these merits can only be achieved effectively with the introduction of excess silicon. It was found that the time dependent dielectric breakdown (TDDB) of silicon oxynitride depends on the thickness of transition SiON layer [40]. The present method for oxynitride preparation will help to improve the lifetime of TDDB for the second reason stated above. When compared to the oxynitride prepared by N_2O annealing, the current technique has the advantage of high nitrogen content which leads to a greater hardness for hot-carrier irradiation.

5. Conclusion

The aggressive scaling of the MOS structure has called for new reliability requirement in gate dielectric materials. Oxynitride had been proposed for the reliability improvement in MOS devices and was investigated extensively in recent years. This paper reviews the major issues of dielectric traps in oxynitride based on experimental and MINDO/3 simulation results. The trap centers being discussed include:

(a) Paramagnetic defects such as $\equiv Si^{\bullet}$, $\equiv Si{-}O{-}O^{\bullet}$, $\equiv Si_2N^{\bullet}$;
(b) Diamagnetic defects such as $\equiv Si{-}Si\equiv$, $=N{-}H$, dicoordinated center ≡Si:;
(c) Neutral defects such as $\equiv SiO^{\bullet}$, =Si:, ≡SiOH, $\equiv Si{-}O{-}O{-}Si\equiv$;
(d) Charged defects such as $\equiv Si^{\bullet}\ ^{+}Si\equiv$ (E′ center in SiO_2), $\equiv Si_2N$: (electron captured by $\equiv Si_2N^{\bullet}$ defect in oxynitride);
(e) Intrinsic defects such as $\equiv Si^{\bullet}$, $=N{-}N=$, $\equiv Si{-}O{-}O{-}Si\equiv$, =Si:, and
(f) Extrinsic defects such as ≡SiH, $\equiv Si_2NH$, ≡SiOH.

Amongst these defects, the paramagnetic defects $\equiv SiO^{\bullet}$ and $\equiv Si_2N^{\bullet}$ which are responsible to the 1.9 ± 2 eV

PL is still significant in oxynitride. However, since the silicon atoms in these defects can be randomly coordinated by different number of oxygen and nitrogen atoms, i.e. $O_{3-\beta}N_{\beta}SiO^{\bullet}$ or $O_{3-\beta}N_{\beta}SiN^{\bullet}$ a slight different peak energy from the conventional R-center in silicon oxide is found and the energy and width of the PL peak depend on the processing conditions. The density of P_b center at the SiO_2/Si interface can be reduced greatly with thermal nitridation as the Si—Si bonds and the silicon dangling bonds ($\equiv Si^{\bullet}$) will be removed with this nitrogen incorporation. However, the $\equiv Si—Si\equiv$ defects will be regenerated with silicon nitride oxidation. Regarding the dicoordinated Si center (=Si:), as the Si atom in oxynitride could be coordinated by two O atoms (O_2Si:), two N atoms (N_2Si:) or and by one Si and one O atom (NOSi:), small shifts in peak energy of the PL and CL studies were found. This dicoordinated Si center is responsible to the positive charge accumulation in MOS devices during ionizing irradiation. Due to the fabrication method, most of the defects in oxynitride are tied to the hydrogen and is the major sources for hot-carrier induced related trap generation in nitrided oxide films. Minimizing the hydrogen incorporation is of vital important for a high reliable oxynitride film for advanced MOS devices applications. With this connection, a new oxynitride preparation method with low hydrogen content and high nitrogen content is proposed.

Acknowledgements

This work is partially supported by research project no. 7001134 of City U.

References

[1] Timp G, Bude J, Baumann F, et al. Microelectron Reliab 2000;40:557.
[2] Degraeve R, Kaczer B, Groeseneken G. Microelectron Reliab 2000;40:697.
[3] Fazan PC, Ditali A, Dennison CH, Rhodes HE, Chan HC, Liu YC. J Electrochem Soc 1991;138:2052.
[4] Minami S, Kamigaki Y. IEEE Trans Electron Devices 1993;40:2011.
[5] Gritsenko VA, Wong H, Xu JB, Kwok RM, Petrenko IP, Zaitsev BA, et al. J Appl Phys 1999;86:3234.
[6] Stadler A, Genchev I, Bergmaier A, Dollinger G, Petrova-Koch V, Hansch W, et al. Microelectron Reliab 2001;41:977.
[7] Gritsenko VA, Svitasheva SN, Petrenko IP, Wong H, Xu JB, Wilson IH. J Electrochem Soc 1999;146:780.
[8] Gritsenko VA, Petrenko IP, Svitasheva SN, Wong H. Appl Phys Lett 1998;72:462.
[9] Morokov YN, Novikov YN, Gritsenko VA, Wong H. Microelectron Eng 1999;48:175.
[10] Wong H, Yang BL, Cheng YC. Appl Surf Sci 1993;72:49.
[11] Wong H, Cheng YC. J Appl Phys 1990;67:7132.
[12] Lucovsky G, Philips JC. Microelectron Eng 1999;48:291.
[13] Colquhoun I, Wild S, Grieveson, Jack KH. Proc Brit Ceram Soc 1973;22:207.
[14] Hori T, Iwasaki H, Tsuji K. IEEE Trans Electron Devices 1989;ED-36:340.
[15] Skuja L. J Non-Cryst Solids 1994;167:229.
[16] Warren WL, Lenahan PM, Curry SE. Phys Rev Lett 1990;65:207.
[17] Yount JT, Lenahan PM. J Non-Cryst Solids 1993;164–166:1069–72.
[18] Chaiyasena IA, Lenahan PM, Dunn GJ. Appl Phys Lett 1984;58:2141.
[19] Robertson J, Powell MJ. Appl Phys Lett 1984;44:415.
[20] Kirk CT. J Appl Phys 1979;50:4190.
[21] Warren WL, Robertson J, Kanicki J. Appl Phys Lett 1993;63:2685.
[22] Gritsenko VA. Electronic structure and optical properties of silicon nitride. In: Silicon nitride in electronics. New York: Elsevier; 1988.
[23] Matsuoka T, Taguchi S, Phtsuka H, Taniguchi K, Hamaguchi C, Kakimoto S, et al. IEEE Trans Electron Devices 1998;43:1364.
[24] Lenahan PM, Dressendorfer PV. J Appl Phys 1984;55:3495.
[25] Edvards AH, Pickard JA, Stahlbish RE. J Non-Cryst Solids 1994;179:148.
[26] Gritsenko VA, Shavalgin JG, Pundur PA, Wong H, Lau WM. Microelectron Reliab 1999;39:715.
[27] Pundur PA, Shavalgin JG, Gritsenko VA. Phys Stat Sol A 1986;94:K107.
[28] Baumvol IJR, Stedile FC, Ganem JJ, Trimaille I, Rigo S. J Electrochem Soc 1996;143:1426.
[29] Wong H, Cheng YC. J Appl Phys 1993;74:7364.
[30] Hori T, Iwasaki H. Appl Phys Lett 1988;52:736–8.
[31] Beichele M, Bauer AJ, Ryssel H. Microelectron Reliab 2000;40:723.
[32] Gritsenko VA, Kwok WM, Wong H, Xu JB, in press.
[33] Gusev EP, Lu HC, Garfunkel EL, Gustaffson T, Green ML. IBM Res Develop 1999;43:1.
[34] Green ML, Brasen D, Evans-Lutterodt KW, Feldman LC, Krisch K, Lennard W, et al. Appl Phys Lett 1994;65:848.
[35] Tobin PJ, Okada Y, Ajuria SA, Lakhotia V, Feil WA, Hedle RI. J Appl Phys 1994;75:1811.
[36] Gonon N, Gagnaire A, Barbier D, Glachant A. J Appl Phys 1994;76:5242.
[37] Lu ZH, Tay SP, Cao R, Pianetta A. Appl Phys Lett 1995;67:2836.
[38] Cerefolini GF, Camalleri M, Galati C, Lorenti S, Renna L, Viscuso O, et al. Appl Phys Lett 2001;79:2378.
[39] Wong H, Poon MC, Gao Y, Kok TCW. J Electrochem Soc 2001;148:G275.
[40] Eriguchi K, Harada Y, Niwa M. Microelectron Reliab 2001;41:587.